

# Probing Neutrino Oscillations in Supersymmetric Models at the Large Hadron Collider

F. de Campos,<sup>1,\*</sup> O. J. P. Éboli,<sup>2,†</sup> M. Hirsch,<sup>3,‡</sup> M. B.  
Magro,<sup>4,5,§</sup> W. Porod,<sup>6,3,¶</sup> D. Restrepo,<sup>7,\*\*</sup> and J. W. F. Valle<sup>3,††</sup>

<sup>1</sup>*Departamento de Física e Química, Universidade Estadual Paulista, Guaratinguetá, SP, Brazil*

<sup>2</sup>*Instituto de Física, Universidade de São Paulo, São Paulo, SP, Brazil.*

<sup>3</sup>*AHEP Group, Instituto de Física Corpuscular – C.S.I.C./Universitat de València  
Edificio Institutos de Paterna, Apartado Postal 22085, E-46071 Valencia, Spain*

<sup>4</sup>*Instituto de Física, Universidade de São Paulo, São Paulo – SP, Brazil.*

<sup>5</sup>*Centro Universitário Fundação Santo André, Santo André, SP, Brazil.*

<sup>6</sup>*Institut für Theoretische Physik und Astronomie, Universität Würzburg, Germany*

<sup>7</sup>*Instituto de Física, Universidad de Antioquia, Colombia*

The lightest supersymmetric particle may decay with branching ratios that correlate with neutrino oscillation parameters. In this case the CERN Large Hadron Collider (LHC) has the potential to probe the atmospheric neutrino mixing angle with sensitivity competitive to its low-energy determination by underground experiments. Under realistic detection assumptions, we identify the necessary conditions for the experiments at CERN's LHC to probe the simplest scenario for neutrino masses induced by minimal supergravity with bilinear  $R$  parity violation.

PACS numbers: 11.30.Pb,12.60.Jv,14.60.Pq,95.30.Cq

## I. INTRODUCTION

The CERN Large Hadron Collider (LHC) will provide high enough center-of-mass energy to probe directly the weak scale and the origin of mass [1–6]. In addition to its designed potential, here we show how LHC searches for new physics at the TeV region may provide an unexpected opportunity to probe neutrino properties, currently determined only in neutrino oscillation experiments [7], shedding light on some of the key issues in neutrino physics. We illustrate how this works in a class of supersymmetric models where the lepton number is broken, together with the so-called  $R$  parity symmetry [8]. Even when the latter holds as a symmetry at the Lagrangian level, as in some SO(10) unification schemes,  $R$  parity breaking may be driven spontaneously by a nonzero vacuum expectation value of an SU(3)  $\otimes$  SU(2)  $\otimes$  U(1) singlet sneutrino [9–12]. In this case the low-energy theory is no longer described by the minimal supersymmetric standard model, but contains new  $R$  parity violating interactions [13–15]. The simplest realization of this scenario leads to an effective model with bilinear violation of  $R$  parity [16–20]. The latter constitutes the minimal way to break  $R$  parity in the minimal supersymmetric standard model and provides the simplest intrinsically supersymmetric way to induce neutrino masses [21–24]. Its main feature is that it relates lightest supersymmetric particle (LSP) decay properties and neutrino mixing angles [25–27].

Here we demonstrate that indeed, under realistic assumptions, the simplest scenario for neutrino masses in su-

---

\*Electronic address: camposc@feg.unesp.br

†Electronic address: eboli@fma.if.usp.br

‡Electronic address: hirsch@ific.uv.es

§Electronic address: magro@fma.if.usp.br

¶Electronic address: porod@physik.uni-wuerzburg.de

\*\*Electronic address: restrepo@uv.es

††Electronic address: valle@ific.uv.es

persymmetry (SUSY) with bilinear violation of  $R$  parity can be tested at the LHC in a crucial way and potentially falsified. We identify the regions of minimal supergravity (mSUGRA) parameters, event reconstruction efficiencies and luminosities where the LHC will be able to probe the atmospheric neutrino mixing angle with sensitivity competitive to its low-energy determination by underground experiments, both for 7 and 14 TeV center-of-mass energies.

For the sake of definiteness, we consider the minimal supergravity model supplemented with bilinear  $R$  parity breaking [22–24] added at the electroweak scale; we refer to this scenario as RmSUGRA. In this effective model one typically finds that the atmospheric scale is generated at tree level by a *weak-scale neutralino-exchange seesaw*, while the solar scale is induced radiatively [22]. The LSP lacks a symmetry to render it stable and, given the neutrino mass scales indicated by oscillation experiments, typically decays inside the LHC detectors [22, 23, 25]<sup>1</sup>. As an illustration we depict the neutralino LSP decay length in Fig. 1. We can see from Fig. 1 that the expected decay lengths are large enough to be experimentally resolved, leading to displaced vertex events [33, 34].

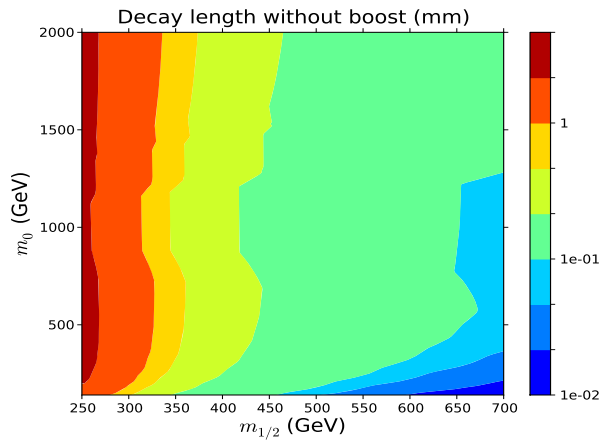


Figure 1:  $\tilde{\chi}_1^0$  decay length in the plane  $m_0, m_{1/2}$  for  $A_0 = -100$  GeV,  $\tan \beta = 10$  and  $\mu > 0$ .

More strikingly, one finds that in such a RmSUGRA model one has a strict correlation between neutralino decay properties measurable at high-energy collider experiments and neutrino mixing angles determined in low-energy neutrino oscillation experiments, that is

$$\tan^2 \theta_{\text{atm}} \simeq \frac{BR(\tilde{\chi}_1^0 \rightarrow \mu^\pm W^\mp)}{BR(\tilde{\chi}_1^0 \rightarrow \tau^\pm W^\mp)}. \quad (1)$$

The derivation of Eq. (1) can be found in [25]. In short, the relation between the neutralino decay branching ratio and the low-energy neutrino angle in the bilinear model can be understood in the following way. At tree-level in RmSUGRA the neutrino mass matrix is given by [22]

$$m_{eff} = \frac{M_1 g^2 + M_2 g'^2}{4 \det(\mathcal{M}_{\chi^0})} \begin{pmatrix} \Lambda_e^2 & \Lambda_e \Lambda_\mu & \Lambda_e \Lambda_\tau \\ \Lambda_e \Lambda_\mu & \Lambda_\mu^2 & \Lambda_\mu \Lambda_\tau \\ \Lambda_e \Lambda_\tau & \Lambda_\mu \Lambda_\tau & \Lambda_\tau^2 \end{pmatrix} \quad (2)$$

where  $\Lambda_i = \mu v_i + v_D \epsilon_i$  and  $\epsilon_i$  and  $v_i$  are the bilinear superpotential parameters and scalar neutrino vacuum expectation value, respectively. Equation (2) is diagonalized by two angles; the relevant one for this discussion is the angle  $\tan \theta_{23} = -\frac{\Lambda_\mu}{\Lambda_\tau}$ . One can understand this tree-level mass as a seesaw-type neutrino mass with the right-handed neutrino and the Yukawa couplings of the ordinary seesaw replaced by the neutralinos of the minimal supersymmetric

<sup>1</sup> We may add, parenthetically, that such schemes require a different type of dark matter particle, such as the axion [28]. Variants with other forms of supersymmetric dark matter, such as the gravitino [29–32], are also possible.

standard model and couplings of the form  $c\Lambda_i$ , where  $c$  is some combination of (generation independent) parameters. These couplings, which determine (the generation structure of) the neutrino mass matrix, also determine the couplings  $\chi_i^0 - l_i^\pm - W^\mp$  and  $\chi_i^\pm - \nu_i - W^\mp$  [25]. Taking the ratio of decays to different generations the prefactors  $c$  drop out and one finds Eq. (1), when the angle  $\tan\theta_{23}$  is identified with the atmospheric neutrino angle. One-loop corrections tend to modify this relation, but, as long as the loop corrections are smaller than the tree-level neutrino mass, Eq. (1) is a good approximation [25].

In other words, as seen in Fig. 2, the LSP decay pattern is predicted by the low-energy measurement of the atmospheric angle [21, 25], currently determined by underground low-energy neutrino experiments [7], as

$$\sin^2\theta_{\text{atm}} = 0.50_{-0.06}^{+0.07}$$

the 2 and 3  $\sigma$  ranges being 0.39–0.63 and 0.36–0.67, respectively.

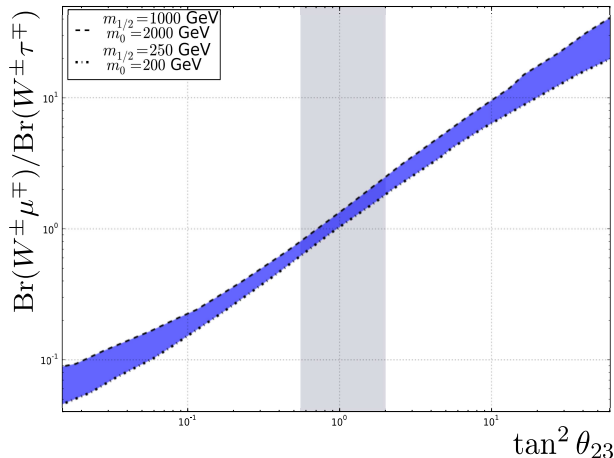


Figure 2: Ratio of  $\tilde{\chi}_1^0$  decay branching ratios,  $\text{Br}(\tilde{\chi}_1^0 \rightarrow \mu q' \bar{q})$  over  $\text{Br}(\tilde{\chi}_1^0 \rightarrow \tau q' \bar{q})$  in terms of the atmospheric angle in bilinear  $R$  parity violation [25]. The shaded bands include the variation of the model parameters in such a way that the neutrino masses and mixing angles fit the required values within  $3\sigma$ .

In this paper we show how a high-energy measurement of LSP decay branching ratios at the LHC allows for a redetermination of  $\theta_{\text{atm}}$  and hence a clear test of the model. We provide quantitative estimates of how well this ratio of branchings should be measured at LHC in order to be competitive with current oscillation measurements. This issue has already been addressed but only at the parton level, using some semirealistic acceptance and reconstruction cuts, and for just one specific mSUGRA point [35].

## II. FRAMEWORK OF OUR ANALYSIS

Our goal is to present a more detailed analysis of the LHC potential to measure the LSP branching ratios required to test the relation shown in Eq. (1), going beyond the approximations made in the previous work of Ref. [35]. The generation of the supersymmetric spectrum and decays in the scope of the RmSUGRA model was carried out using the SPheno package [36]<sup>2</sup>. The event generation was done employing PYTHIA [37] with the RmSUGRA particle properties being passed into it in the SUSY Les Houches accord (SLHA) format [38, 39]. Jets were defined using the subroutine PYCELL with a cone size of  $\Delta R = 0.4$ .

<sup>2</sup> An updated version including bilinear  $R$  parity violation can be obtained at <http://www.physik.uni-wuerzburg.de/~porod/SPheno.html>.

A striking property of RmSUGRA models is the existence of displaced vertices associated to the LSP decay [34]. We use the detached vertices to probe the LSP branching ratio relation Eq. (1). In order to mimic the LHC potential to study displaced vertices we use a toy detector based on the ATLAS technical proposal [3].

We begin our analysis demanding that the events pass some basic requirements to guarantee that they will be triggered by the experimental collaborations. This is done because the LHC experiments have not defined so far any specific strategy to trigger displaced vertices with such high invariant mass, therefore, we restricted our analysis to events that would be accepted by the ongoing analyses. We accept events passing at least one of the following requirements, denoted as cut **C1**,

1. the event has one isolated electron or a photon with  $p_T > 20$  GeV;
2. the event has one isolated muon with  $p_T > 6$  GeV;
3. the event has two isolated electrons or photons with  $p_T > 15$  GeV;
4. the event has one jet with  $p_T > 100$  GeV;
5. the event has missing transversal energy in excess of 100 GeV.

Next, in cut **C2**, we require that at least one of the neutralinos in the event decays beyond the primary vertex point, that is, outside an ellipsoid [34]

$$\left(\frac{x}{5\delta_{xy}}\right)^2 + \left(\frac{y}{5\delta_{xy}}\right)^2 + \left(\frac{z}{5\delta_z}\right)^2 = 1, \quad (3)$$

where the  $z$  axis is taken along the beam direction. We made a conservative assumption, since we are not performing a detailed detector simulation, that the ellipsoid dimensions are 5 times the ATLAS expected resolutions in the transverse plane ( $\delta_{xy} = 20 \mu\text{m}$ ) and in the beam direction ( $\delta_z = 500 \mu\text{m}$ ), in order to ensure that the neutralino displaced vertex is distant of the primary vertex. We also demand that all tracks must be initiated inside the pixel inner detector within a radius of 550 mm and  $z$  axis length of 800 mm. A detached vertex complying with these requirements we called *signal vertex*.

In order to check relation Eq. (1) we looked for detached vertices presenting a  $W$  associated to them and we must isolate the LSP decays into  $W\mu$  and  $W\tau$ . Moreover we consider only hadronic final states of the  $W$  as a necessary condition for the identification of the lepton flavor. In cut **C3**, which is designed for the  $W$  reconstruction, we require two jets with charged tracks intersecting the neutralino resolution ellipsoid, and invariant mass between 60 and 100 GeV. In order to be sure that the  $W$  reconstruction is clean, we further impose that the axes of other jets of the event to be outside of a cone  $\Delta R = 0.8$  of the  $W$  jets' axes. Note that this cut should eliminate standard model (SM) backgrounds coming from displaced vertices associated to  $b$ 's or  $\tau$ 's. To guarantee a high quality in the reconstruction of the displaced vertices we impose that the  $W$  decay jets must be central, having pseudorapidities  $|\eta| < 2.5$ ; this constitutes our cut **C4**. The events passing the above requirements most probably originate from LSP decay, having basically no sizable standard model background, except for instrumental backgrounds and beam-gas interactions.

A signal vertex is classified as originating from the LSP decay into a  $\mu W$  pair if it presents a  $\mu^\pm$  and a hadronically decaying  $W$  stemming from the displaced vertex with transverse momentum  $p_T > 6$  GeV and  $|\eta| < 2.5$ . In the  $\tau^\pm$  case we demanded that the  $\tau^\pm$  associated to a detached  $W$  possesses  $p_T > 20$  GeV and  $|\eta| < 2.5$ . These requirements are called **C5**.

Detecting taus is somewhat more complicated than detecting muons, so one needs to be more careful in reconstructing the  $\tau W$  pair displaced vertex. The following criteria, denoted **C6**, are used to separate the detached vertices exhibiting a  $\tau^\pm$  through its 1- and 3-prong decay modes. We check also that the secondary displaced vertex from tau decay does not spoil the signal vertex; *i.e.*, we verify that the tau decay products point towards the LSP decay

vertex within the experimental resolution. We define the neutralino resolution ellipsoid as the ellipsoid centered at the displaced vertex position of neutralino,  $v_1$ , with axes  $\delta_{xy} = 12 \mu\text{m}$  and  $\delta_z = 77 \mu\text{m}$  based on ref. [3]. Let  $\mathbf{p}_{\text{prong}}$  be the momentum of either 1-prong tau decay or the sum of momenta of the 3-prong decays. Let also  $v_2$  be the position of the secondary vertex coming from  $\tau$ . We verify whether the line along  $\mathbf{p}_{\text{prong}}$ , crossing  $v_2$  intersects the neutralino resolution ellipsoid. For this we require that for each  $\tau$ , the discriminant of quadratic equation for parameter  $t$

$$\sum_i^2 \left( \frac{p_{\text{prong}}^i t + v_2^i - v_1^i}{\delta_{xy}} \right)^2 + \left( \frac{p_{\text{prong}}^3 t + v_2^3 - v_1^3}{\delta_z} \right)^2 - 1 = 0 \quad (4)$$

be equal to or greater than zero. In previous [35] analysis only 3-prong tau decays modes were considered.

An additional cut **C7** was applied to 3-prong tau events, *i.e.* we also require that one of the prongs has a transverse momentum  $p_T > 9 \text{ GeV}$  while the other two have  $p_T > 2 \text{ GeV}$ . In addition we check if all prongs lie within a cone radius of  $\Delta R < 0.2$  around the tau direction obtained from the prongs' tracks.

Finally we require that the signal lepton ( $\mu$  or  $\tau$ ) be isolated; cut **C8**.  $\mu$  isolation demands that there are no other tracks whose total transverse energy satisfies  $E_T > 5 \text{ GeV}$  within a cone  $\Delta R > 0.3$ . The  $\tau$  was required to be isolated using the same criteria as for the muon, but for an annulus of outer radius  $\Delta R = 0.4$  and inner radius  $\Delta R = 0.1$ . Isolation of the leptons is a needed requirement to eliminate events presenting leptons generated inside jets and constitutes an important cut to reduce potential backgrounds.

### III. RESULTS AND DISCUSSION

In order to access the effects of the above defined cuts **C1–C8** we present detailed information on their effects for the mSUGRA SPS1a benchmark point [40] characterized by  $m_{1/2} = 250 \text{ GeV}$ ,  $m_0 = 100 \text{ GeV}$ ,  $A_0 = -100 \text{ GeV}$ ,  $\tan\beta = 10$ , and  $\text{sgn}(\mu) = +1$ . This allows us to compare our results with the one previously obtained in [35]. For the default solution of **SPheno** to the neutrino masses and mixings, the relevant neutralino branching ratios are

$$\begin{aligned} \text{BR}(\tilde{\chi}_1^0 \rightarrow W^\pm \mu^\mp) &= 5.4\% & \text{BR}(\tilde{\chi}_1^0 \rightarrow W^\pm \tau^\mp) &= 6.2\% & \text{BR}(\tilde{\chi}_1^0 \rightarrow Z\nu) &= 1.2\% \\ \text{BR}(\tilde{\chi}_1^0 \rightarrow e^\pm \tau^\mp \nu) &= 11.5\% & \text{BR}(\tilde{\chi}_1^0 \rightarrow \mu^\pm \tau^\mp \nu) &= 24.3\% & \text{BR}(\tilde{\chi}_1^0 \rightarrow \tau^\pm \tau^\mp \nu) &= 36.4\% \\ & & \text{BR}(\tilde{\chi}_1^0 \rightarrow b\bar{b}\nu) &= 14.7\%; & & \end{aligned} \quad (5)$$

with the  $R$  parity parameters being

$$\begin{aligned} \epsilon_1 &= 0.0405 \text{ GeV}, & \epsilon_2 &= -0.0590 \text{ GeV}, & \epsilon_3 &= 0.0506 \text{ GeV}, \\ v_1 &= -0.0027 \text{ GeV}, & v_2 &= 0.0042 \text{ GeV}, & v_3 &= -0.0033 \text{ GeV}. \end{aligned}$$

Furthermore, for this choice of parameters the neutralino decay length is  $c\tau = 1.1 \text{ mm}$ , and it travels an average of  $4.4 \text{ mm}$  in the laboratory.

From Table I we see that the vast majority of the events pass the trigger requirements **C1**, as expected. For the SPS1a SUSY point, the LSP decay length is sufficiently long to guarantee that a sizeable fraction of its decays take place away from the primary vertex; this reflects as a high efficiency for passing the cut **C2**. We have focused our attention to events presenting a  $W^\pm$  decaying into two jets through **C3**. It is interesting to notice that 63% of the  $W$  hadronic decays are in the form of two jets. Additional suppression of the signal by **C3** comes from the matching of the sum of momenta of the charged tracks pointing to the detached vertex and the jets reconstructed using **PYTHIA**. To further illustrate the  $W$  decay, we present in Fig. 3 the jet–jet invariant mass distribution. As we can see, this distribution is clearly peaked around the  $W$  mass and a good fraction of the two jets reconstructed as associated to the LSP decay pass the cut **C3**. The observed high efficiency of cut **C4** shows that the  $W$ 's produced in the LSP decay are rather central.

cut	$N_\mu$	$N_\tau$	$N_{\tau \rightarrow \text{all}}^{1\text{-prong}}$	$N_{\tau \rightarrow \text{hadron}}^{1\text{-prong}}$	$N_\tau^{3\text{-prong}}$
<b>C1</b>	0.996	0.968	0.816	0.475	0.058
<b>C2</b>	0.923	0.898	0.757	0.440	0.055
<b>C3</b>	0.391	0.407	0.344	0.199	0.025
<b>C4</b>	0.369	0.385	0.325	0.188	0.024
<b>C5</b>	0.230	0.248	0.211	0.121	0.024
<b>C6+C7</b>	0.230	0.078	0.057	0.033	0.014
<b>C8</b>	0.102	0.015	0.014	0.009	0.001

Table I: Fraction of events passing the successive cuts **C1**–**C8** used for the event reconstruction at the SPS1a mSUGRA point.

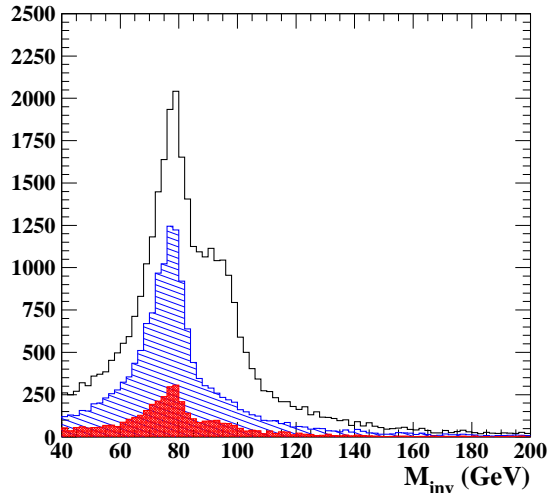


Figure 3: From top to bottom:  $\tilde{\chi}_1^0 \rightarrow jjX$  without cuts, with cut on lepton isolation ( $\mu$  or  $\tau$ ) and with all other cuts leaving free the invariant mass range.

We also learn from Table I that detached vertices presenting a  $W$  possess around 60% of the time an energetic  $\mu^\pm$  or  $\tau^\pm$  complying with **C5**. Moreover the cuts **C6** and **C7**, which ensure the quality of the  $\tau$  reconstruction, reduce significantly the number of  $W^\pm\tau^\mp$  events. Finally the isolation cut **C8** turns out to be quite important significantly reducing the signal.

For the parameter point SPS1a, the expected efficiencies for the reconstruction of  $\mu W$  and  $\tau W$  decays are 0.107 and 0.0098 respectively, where in the last we have added 1- and 3-prong hadronic decays. When the  $\tau$  decays into a  $\mu$  and neutrinos, the event was computed as being a  $\mu W$  decay if the  $\mu$  passes the cuts. This was included appropriately in our calculations. Taking into account the total SUSY production cross section (41 pb) at 14 TeV, an integrated luminosity of  $100 \text{ fb}^{-1}$  and these efficiencies we anticipate that the number of observed  $\mu W$  and  $\tau W$  events after cuts to be

$$N_\mu = 32000 \qquad N_\tau^{\text{hadron}} = 3382$$

where  $N_\tau^{\text{hadron}} = N_{\tau \rightarrow \text{hadron}}^{1\text{-prong}} + N_\tau^{3\text{-prong}}$ . Therefore, the statistical accuracy of the ratio  $R = BR(\tilde{\chi}_1^0 \rightarrow \mu^\pm W^\mp) / BR(\tilde{\chi}_1^0 \rightarrow \tau^\pm W^\mp)$  is expected to be  $\sigma(R)/R = \sqrt{1/N_\mu + 1/N_\tau} \approx 0.015$ . In the case one takes into account only the three-prong decays of the tau, as in Ref. [35], the statistical error of this ratio increases to  $\approx 0.053$ . Moreover, as expected, there is a degradation of the accuracy in the determination of this ratio of branching ratios in a more realistic analysis; the result obtained in [35] is  $\simeq 0.028$ .

In the evaluation of the above efficiencies we have not taken into account multiple interactions at the LHC as needed for the high luminosity run. Therefore, we reevaluated the detection efficiencies for muons and taus with multiple interactions switched on in PYTHIA. We found that these efficiencies were only slightly degraded by the occurrence of pileup, that is, we obtained that the efficiencies for muon reconstruction are reduced to 0.102 and for tau are 0.008 68 in hadronic mode and 0.000 94 in the 3-prong mode. In our analyses we took into account the effect of multiple interactions.

For the sake of comparison, we present a detailed analysis for a different mSUGRA point that is  $m_{1/2} = 500$  GeV,  $m_0 = 500$  GeV,  $A_0 = -100$  GeV,  $\tan\beta = 10$ , and  $\text{sgn}(\mu) = +1$ . Once again using SPheno, we obtain that the neutralino branching ratios larger than 1% are:

$$\begin{aligned} \text{BR}(\tilde{\chi}_1^0 \rightarrow W^\pm \mu^\mp) &= 22.9\%, & \text{BR}(\tilde{\chi}_1^0 \rightarrow W^\pm \tau^\mp) &= 25.2\%, & \text{BR}(\tilde{\chi}_1^0 \rightarrow Z\nu) &= 25.1\%, \\ \text{BR}(\tilde{\chi}_1^0 \rightarrow \nu h^0) &= 16.9\%, & \text{BR}(\tilde{\chi}_1^0 \rightarrow \tau^\pm \tau^\mp \nu) &= 3.4\%, & \text{BR}(\tilde{\chi}_1^0 \rightarrow b\bar{b}\nu) &= 2.9\%; \end{aligned}$$

and the corresponding  $R$  parity parameters are

$$\begin{aligned} \epsilon_1 &= 0.1507 \text{ GeV}, & \epsilon_2 &= -0.1507 \text{ GeV}, & \epsilon_3 &= 0.1507 \text{ GeV}, \\ v_1 &= -0.0056 \text{ GeV}, & v_2 &= 0.0058 \text{ GeV}, & v_3 &= -0.0054 \text{ GeV}. \end{aligned}$$

As we can see, the neutralino LSP decays are dominated by the two-body ones, in contrast with the SPS1a point where the three-body decays mediated by light scalars are dominant. Because of its heavier spectrum, the total SUSY production for this parameter point is smaller than the SPS1a one; however, the cross section loss is partially compensated by the higher branching ratios into  $\mu W$  and  $\tau W$ .

The total cross section for this case is 832.0 fb and our analyses indicate that the reconstruction efficiency for  $\mu W$  decays is 0.203 while the  $\tau W$  decays are reconstructed with an efficiency of 0.035, where we did not take into account pileup. The inclusion of this effect leads to a tiny reduction of the reconstruction efficiencies that become 0.199 for  $\mu W$  and 0.033 for  $\tau W$ . On the other hand the efficiency for reconstructing a  $\tau W$  event in the 3-prong mode is 0.012. Notice that these efficiencies are larger for this mSUGRA point than for the SPS1a because the neutralino is heavier and, consequently, its decay products are more energetic and pass the cuts more easily. The expected total number of reconstructed events after cuts for this SUSY point is  $N_\mu = 5171$  and  $N_\tau^{\text{hadron}} = 933$  where we have included the pileup effects. Therefore, the expected statistical error on the ratio  $R$  becomes  $\approx 0.036$ , or  $\approx 0.056$  when we only use 3-prong taus as in [35]. As we can see, the statistical error on the ratio  $R$  increases as  $m_{1/2}$  (LSP mass) increases due to the reduction of the SUSY production cross section despite the increase in the detection efficiencies.

We evaluated the reconstruction efficiencies as a function of  $m_0 \otimes m_{1/2}$  for  $A_0 = -100$  GeV,  $\tan\beta = 10$  and  $\text{sgn}(\mu) = +1$  and our results are depicted in Fig. 4. As we can see from the left panel of this figure, the  $\mu W$  decays exhibit a high reconstruction efficiency, *i.e.*, between 10% and 20%, in a large area of the parameter space, degrading only at large  $m_{1/2}$ . On the other hand, the  $\tau W$  reconstruction (see right panel of Fig. 4) is at most 3.5%, indicating that the statistical error on the ratio  $R$  is going to be dominated by these events.

We present in Fig. 5 the attainable precision  $\sigma(R)/R$  with which the correlation  $R$  can be measured as a function of  $m_0 \otimes m_{1/2}$  for  $A_0 = -100$  GeV,  $\tan\beta = 10$ , and  $\text{sgn}(\mu) = +1$  for an integrated luminosity of  $100 \text{ fb}^{-1}$  and a center-of-mass energy of 14 TeV. We require in all plots that at least 5 events of reconstructed taus are observed. In the left panel of this figure we present the expected statistical error on the ratio  $R$  assuming no systematic errors on the determination of the reconstruction efficiencies, while in the right panel we consider a more conservative scenario, where we anticipate a systematic error of 10% in each of the reconstruction efficiencies. One can see from this panel that the precision drops as  $m_{1/2}$  grows since the neutralino production rates from squark/gluino cascade decays also decrease with increasing  $m_{1/2}$  values. Therefore, if the systematic errors of the efficiency determination are negligible the LHC collaborations should be able to probe with a very good precision ( $\lesssim 10\%$ ) the ratio  $R$  for  $m_{1/2} \lesssim 650$  GeV, which correspond to an LSP mass up to  $\simeq 270$  GeV. The inclusion of systematic errors at the level assumed in the



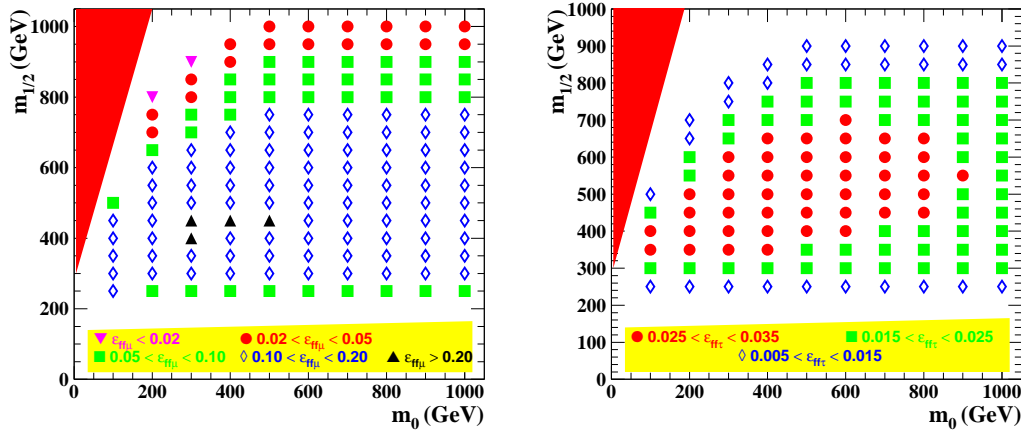


Figure 4: Reconstruction efficiencies of  $\mu W$  (left panel) and  $\tau W$  events (right panel) as a function of  $m_0 \otimes m_{1/2}$  for  $A_0 = -100$  GeV,  $\tan \beta = 10$  and  $\text{sgn}(\mu) = +1$  including the effect of pileup. The red (dark shaded) area corresponds to the region where stau is the LSP, while the yellow (light shaded) area represents the region excluded by LEP.

right panel of Fig. 5 increases the uncertainty in  $R$ ; however, it is still possible to perform an accurate test of the RmSUGRA scenario.

Note that in Fig. 5 we also present results for the 7 TeV run of the LHC. For this case one can see that the LHC has a much more limited capability of probing the ratio  $R$ , since the reach of this run covers only up to  $m_{1/2} \lesssim 300$  GeV. Still, although large, the statistical errors in this region [ $0.3 \lesssim \sigma(R)/R \lesssim 0.5$ ], due mainly to the small anticipated integrated luminosity, which we have taken to be  $1 \text{ fb}^{-1}$ , allow a determination of the atmospheric angle comparable to that obtained at low energies.

In the left panel of Fig. 6 we show the dependence of the attained precision as a function of the neutralino mass for luminosities of 2, 10, and 100  $\text{fb}^{-1}$ . For small neutralino masses the SUSY production cross section is large enough to guarantee that the statistical errors are small; therefore, the uncertainty on the ratio  $R$  is dominated by the assumed systematic errors on the reconstruction efficiencies, even for an integrated luminosity of 2  $\text{fb}^{-1}$ . As the accumulated luminosity increases the LHC experiments will be able to probe higher neutralino masses; however, the precision worsens due to the increase of statistical errors. We can also see clearly that increasing the luminosity allows a more precise measurement of  $R$  as expected. Moreover, one can probe LSP masses up to 250 (320 or 370) GeV for an integrated luminosity of 2 (10 or 100)  $\text{fb}^{-1}$ .

From the right panel of Fig. 6 we estimate the luminosity needed to measure  $R$  with a given precision for several LSP masses. For instance, let us consider  $m_{\tilde{\chi}_1^0} = 250$  GeV. In this case  $R$  can only be measured with a precision  $\sigma(R)/R \simeq 50\%$  with 2  $\text{fb}^{-1}$ , while this error can be brought down to 20%, *i.e.*, close to the limit set by the systematic uncertainties, with 50  $\text{fb}^{-1}$ .

#### IV. CONCLUSIONS

We have demonstrated how the LHC may have the potential of probing neutrino mixing angles with sensitivity competitive to their low-energy determination by oscillation experiments. This analysis was carried out, for the sake of concreteness, in the simplest scenario for neutrino masses induced by minimal supergravity with  $R$  parity violation as framework. In this class of models, the smoking gun for the neutrino mass generation mechanism is the ratio of



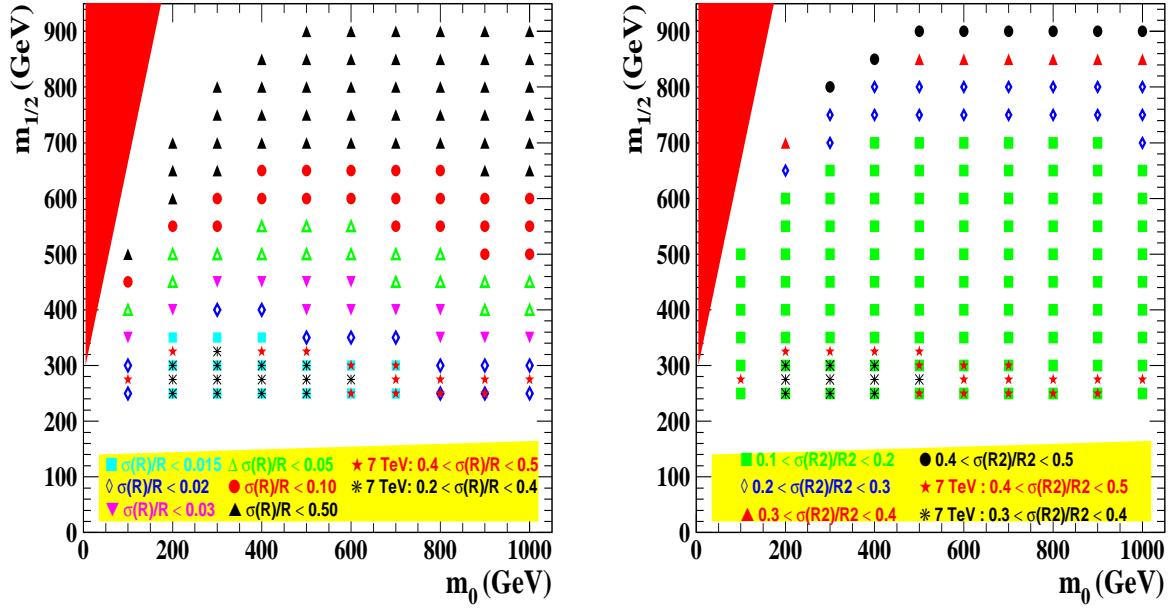


Figure 5: Precision in the determination of the ratio  $R$  in the plane  $m_{1/2} \times m_0$  for a luminosity of  $100 \text{ fb}^{-1}$ , center-of-mass energy of 14 TeV,  $A_0 = -100 \text{ GeV}$ ,  $\tan\beta = 10$ , and  $\text{sgn}(\mu) = +1$ . In the right (left) panel we did (not) include a possible systematic uncertainty in the extraction of the efficiencies for the channels  $\mu W$  and  $\tau W$ . The stars in the right panel represent the results for the 7 TeV run with an integrated luminosity of  $1 \text{ fb}^{-1}$ . The shaded areas represent the same as in Fig. 4.

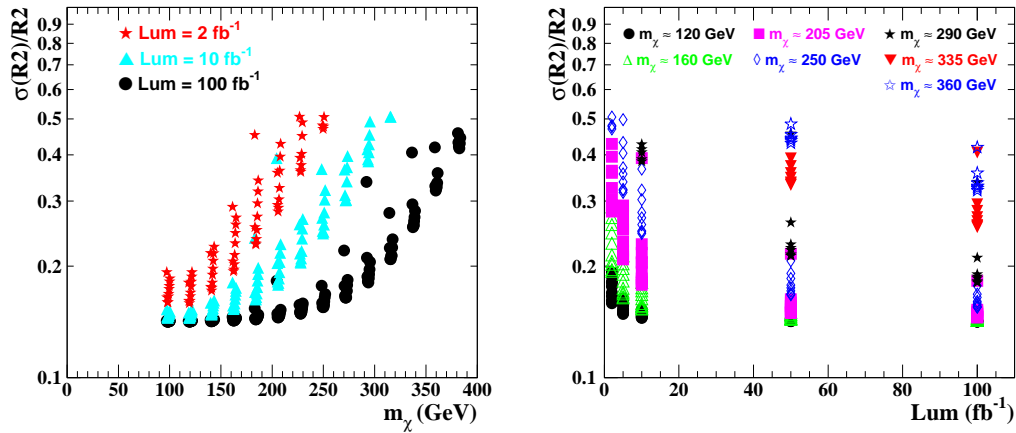


Figure 6: The left panel displays the achievable precision in the ratio  $R$  as a function of the neutralino mass  $m_{\tilde{\chi}_1^0}$  for luminosities of 2, 10, and  $100 \text{ fb}^{-1}$  at 14 TeV whereas the right panel contains the foreseen statistical error on  $R$  as a function of the integrated luminosity for several LSP masses.

branching fractions of neutralino decaying into  $\mu W$  and  $\tau W$ , as this fraction is related to the atmospheric neutrino mixing angle in RmSUGRA models.

Under realistic detection assumptions we have made a detailed analysis of the reconstruction of neutralino decays, as well as of the cuts needed to characterize the signal. After that we determined the attainable precision on the measurements of the ratio  $R$  given in Eq. (1). Comparing with a previous parton level study, we improved the reconstruction efficiencies of muons as well as taus.

We showed that the 7 TeV run of the LHC will have a somewhat weak potential for probing the RmSUGRA model, since it is statistics limited. Still, precisions comparable to the low-energy determination should be reached. In contrast, a 14 TeV run with  $100 \text{ fb}^{-1}$  integrated luminosity will be able to probe a large fraction of the parameter space with a good precision, as seen in Fig. 5. In fact, our analyses suggest that the error on  $R$  will be dominated by the systematic ones on the reconstruction efficiencies of the decay  $\mu W$  and  $\tau W$ , with the statistical errors being under control.

In short, we find that in this case the atmospheric mixing angle may be probed relatively neatly. In fact, a determination of  $R$  within a given error translates into a prediction of the atmospheric mixing angle with an error of very similar size. Needless to say, what we have presented is only one example of a class of LSPs. There are other variant schemes based on alternative supersymmetry and/or  $R$  parity breaking, where other states emerge as LSP and similar correlations to other neutrino mixing angles appear [41–43]. These would, however, require separate dedicated studies. We encourage the particle detector groups ATLAS and CMS to add the test of such possibilities to their physics agenda, as this might lead to a tantalizing synergy between high-energy accelerator and low-energy nonaccelerator searches for new physics. Studies with the real LHC data may also make it possible to probe, at some level, the mass scale characterizing atmospheric neutrino oscillations, as well as the angle characterizing solar neutrino oscillations, an issue to be taken up separately.

## Acknowledgments

Work supported in part by Spanish grants FPA2008-00319/FPA, MULTIDARK Consolider CSD2009-00064 and PROMETEO/2009/091, by European network UNILHC, PITN-GA-2009-237920, by Conselho Nacional de Desenvolvimento Científico e Tecnológico (CNPq), and by Fundação de Amparo à Pesquisa do Estado de São Paulo (FAPESP). F. de Campos thanks USP and IFIC/C.S.I.C. for hospitality. M.B.M. thanks IFIC/C.S.I.C. for hospitality. W.P. is supported by the DFG, Project No. PO-1337/1-1, and by the Alexander von Humboldt Foundation. D.R. is partly supported by Sostenibilidad-UdeA/2009 grant.

- 
- [1] P. Nath *et al.*, Nuclear Physics B (Proc. Suppl.) **200-202**, 185 (2010), [arXiv:1001.2693].
  - [2] S. P. Martin, hep-ph/9709356.
  - [3] ATLAS Collaboration, ATLAS inner detector: Technical design report. Report No. CERN-LHCC-97-16, Vol. 1.
  - [4] J. A. Aguilar-Saavedra *et al.*, Eur. Phys. J. **C46**, 43 (2006), [hep-ph/0511344].
  - [5] G. L. Bayatian *et al.*, J. Phys. **G34**, 995 (2007).
  - [6] The ATLAS, G. Aad *et al.*, arXiv:0901.0512.
  - [7] T. Schwetz, M. Tortola and J. W. F. Valle, New J. Phys. **10**, 113011 (2008), [arXiv:0808.2016]; for a review see M. Maltoni *et al.*, New J. Phys. **6**, 122 (2004).
  - [8] R. Barbier *et al.*, Phys. Rept. **420**, 1 (2005), [hep-ph/0406039].
  - [9] A. Masiero and J. W. F. Valle, Phys. Lett. **B251**, 273 (1990).
  - [10] J. C. Romao, C. A. Santos and J. W. F. Valle, Phys. Lett. **B288**, 311 (1992).
  - [11] J. C. Romao, A. Ioannissyan and J. W. F. Valle, Phys. Rev. **D55**, 427 (1997), [hep-ph/9607401].
  - [12] For a recent review see G. Bhattacharyya and P. B. Pal, Phys. Rev. D **82** 055013 (2010).
  - [13] L. J. Hall and M. Suzuki, Nucl. Phys. **B231**, 419 (1984).

- [14] G. G. Ross and J. W. F. Valle, Phys. Lett. **B151**, 375 (1985).
- [15] J. R. Ellis and *et al.*, Phys. Lett. **B150**, 142 (1985).
- [16] M. A. Diaz, J. C. Romao and J. W. F. Valle, Nucl. Phys. **B524**, 23 (1998), [hep-ph/9706315].
- [17] E. J. Chun, S. K. Kang, C. W. Kim and U. W. Lee, Nucl. Phys. **B544**, 89 (1999), [hep-ph/9807327].
- [18] D. E. Kaplan and A. E. Nelson, JHEP **01**, 033 (2000), [hep-ph/9901254].
- [19] F. Takayama and M. Yamaguchi, Phys. Lett. **B476**, 116 (2000), [hep-ph/9910320].
- [20] T. Banks, Y. Grossman, E. Nardi and Y. Nir, Phys. Rev. **D52**, 5319 (1995), [hep-ph/9505248].
- [21] J. C. Romao, M. A. Diaz, M. Hirsch, W. Porod and J. W. F. Valle, Phys. Rev. **D61**, 071703 (2000), [hep-ph/9907499].
- [22] M. Hirsch, M. A. Diaz, W. Porod, J. C. Romao and J. W. F. Valle, Phys. Rev. **D62**, 113008 (2000), [hep-ph/0004115], Err-ibid. **D65**:119901,2002.
- [23] M. A. Diaz, M. Hirsch, W. Porod, J. C. Romao and J. W. F. Valle, Phys. Rev. **D68**, 013009 (2003), [hep-ph/0302021].
- [24] M. Hirsch and J. W. F. Valle, New J. Phys. **6**, 76 (2004), [hep-ph/0405015].
- [25] W. Porod, M. Hirsch, J. C. Romao and J. W. F. Valle, Phys. Rev. **D63**, 115004 (2001), [hep-ph/0011248].
- [26] S. Y. Choi, E. J. Chun, S. K. Kang and J. S. Lee, Phys. Rev. **D60**, 075002 (1999), [hep-ph/9903465].
- [27] B. Mukhopadhyaya, S. Roy and F. Vissani, Phys. Lett. **B443**, 191 (1998).
- [28] E. J. Chun and H. B. Kim, Phys. Rev. **D60**, 095006 (1999), [hep-ph/9906392].
- [29] S. Borgani, A. Masiero and M. Yamaguchi, Phys. Lett. **B386**, 189 (1996), [hep-ph/9605222].
- [30] F. Takayama and M. Yamaguchi, Phys. Lett. **B485**, 388 (2000), [hep-ph/0005214].
- [31] M. Hirsch, W. Porod and D. Restrepo, JHEP **03**, 062 (2005), [hep-ph/0503059].
- [32] F. Staub, W. Porod and J. Niemeyer, JHEP **01**, 058 (2010), [0907.0530].
- [33] F. de Campos *et al.*, Phys. Rev. **D71**, 075001 (2005), [hep-ph/0501153].
- [34] F. de Campos *et al.*, JHEP **05**, 048 (2008).
- [35] W. Porod and P. Skands, hep-ph/0401077.
- [36] W. Porod, Comput. Phys. Commun. **153**, 275 (2003), [hep-ph/0301101].
- [37] T. Sjostrand, S. Mrenna and P. Skands, JHEP **05**, 026 (2006), [hep-ph/0603175].
- [38] P. Skands *et al.*, JHEP **07**, 036 (2004), [hep-ph/0311123].
- [39] B. Allanach *et al.*, Comp. Phys. Commun. **180**, 8 (2009), [arXiv:0801.0045].
- [40] B. C. Allanach *et al.*, Eur. Phys. J. **C25**, 113 (2002), [hep-ph/0202233].
- [41] D. Restrepo, W. Porod and J. W. F. Valle, Phys. Rev. **D64**, 055011 (2001).
- [42] M. Hirsch, W. Porod, J. C. Romao and J. W. F. Valle, Phys. Rev. **D66**, 095006 (2002), [hep-ph/0207334].
- [43] M. Hirsch and W. Porod, Phys. Rev. **D68**, 115007 (2003), [hep-ph/0307364].